Near threshold J/ψ and Υ photoproduction at JLab and RHIC

Yoshitaka Hatta,[1] Abha Rajan,[1] and Di-Lun Yang[2,3]

[1]*Physics Department, Brookhaven National Laboratory, Upton, New York 11973, USA*
[2]*Faculty of Science and Technology, Keio University, Yokohama 223-8522, Japan*
[3]*Yukawa Institute for Theoretical Physics, Kyoto University, Kyoto 606-8502, Japan*

(Received 6 June 2019; published 29 July 2019)

We update our previous calculation of J/ψ photoproduction near threshold [Y. Hatta and D. L. Yang, Phys. Rev. D **98**, 074003 (2018)] by incorporating the recent developments in theory and the new experimental data from Ali *et al.* [the GlueX Collaboration] at Jefferson Laboratory. We then propose to study the near threshold production of Υ and J/ψ in ultraperipheral pA collisions at RHIC. These processes are sensitive to the gluon condensate in the proton which is related to the proton mass via the QCD trace anomaly. Our result emphasizes the role of gluons in generating the proton mass.

DOI: 10.1103/PhysRevD.100.014032

I. INTRODUCTION

Although it is a well-known fact that the proton has a complex internal structure, much of the confining mechanism that brings the quarks and gluons together to form the proton remains a mystery. In particular, the mass of the proton $M = 0.938$ GeV cannot be explained by the naive sum of current quark masses which only accounts for a tiny fraction of the total mass. The remaining part must come from the nonperturbative dynamics of quarks and gluons. Among various contributions to the proton mass, the role of the QCD trace anomaly has attracted a lot of attention lately. Dedicated experiments to probe the trace anomaly contribution are currently running at Jefferson Laboratory (JLab) [1], and similar experiments are planned at the future Electron-Ion Collider.

Specifically, JLab measures the photoproduction of J/ψ in ep scattering. At low energy, very close to the threshold, the cross section of this process is sensitive to the gluon condensate $\langle P|F^{\mu\nu}F_{\mu\nu}|P\rangle$ in the proton [2] which is closely related to the trace anomaly. However, extracting the value of the condensate from the experimental data is highly nontrivial and subject to large systematic uncertainties. This is because QCD factorization for this process is difficult to establish as it involves the twist-four operator F^2, and in practice one has to employ a nonperturbative model to calculate the cross section. Yet, some models allow for a more systematic treatment of the problem than others. In a previous publication [3], two of the present authors have proposed a holographic approach based on gauge-string duality. In the limit of heavy-quark mass, it has been shown that the cross section is directly related to the so-called gravitational form factors of the proton. Since these form factors can be analyzed by other means (e.g., in lattice QCD simulations), a large part of uncertainties associated with the nonperturbative proton matrix elements can be absorbed into those of the form factors. In [3], the theoretical result was fitted to the 40-year-old experimental data from Cornell [4] and SLAC [5] which were the only available data to compare at that time. The quality of the fit was not satisfactory, especially with the Cornell data which are closer to the threshold. It was not clear whether this was due to the naivety of the model, or perhaps because the old data were not quite accurate.

Very recently, the GlueX Collaboration at JLab has reported new data for the threshold cross section which significantly differ from the Cornell data [6]. Meanwhile, there have been theory developments on the renormalization of the trace anomaly [7,8] as well as the first lattice calculation of the gluon "D-term" gravitational form factors [9]. In view of these, we feel it is necessary to revise the calculations and fits in [3]. This is what we shall do in the first part of this paper.

In the second part, we propose a novel way to measure the gluon condensate in experiments. This is the threshold production of J/ψ and Υ in ultraperipheral pA collisions (UPCs) at RHIC. In UPCs, a heavy nucleus emits almost real photons which interact with the proton electromagnetically. The process thus closely mimics the photoproduction limit of ep scattering and serves as nontrivial cross checks of the experimental results as well as the consistency of the theoretical formalism. Moreover, RHIC can study the Υ production which is energetically not possible at JLab. On the other hand, the high energy of

RHIC obviously makes the study of threshold production technically difficult. We however argue that this is feasible once the forward upgrade of the STAR detector has been completed [10].

II. NUCLEON MASS DECOMPOSITION

The approximate conformal symmetry of the QCD Lagrangian is explicitly broken by the quantum effects. One of the profound consequences of this fact is that the mass of a hadron is directly related to the QCD trace anomaly. For a single hadron state $|P\rangle$ with mass squared $M^2 = P^2$, the QCD energy momentum tensor has the following expectation value:

$$\langle P|T^{\alpha\beta}|P\rangle = 2P^\alpha P^\beta, \tag{1}$$

$$\begin{aligned}\langle P|T^\alpha_\alpha|P\rangle &= \langle P|\left(\frac{\beta(g)}{2g}F^{\mu\nu}F_{\mu\nu} + m(1+\gamma_m(g))\bar\psi\psi\right)|P\rangle \\ &= 2M^2,\end{aligned} \tag{2}$$

where $\beta(g)$ is the beta function of QCD and $\gamma_m(g) = -\frac{1}{m}\frac{\partial m}{\partial \ln \mu}$ is the mass anomalous dimension. The sum over different flavors is implied in $m\bar\psi\psi = \sum_f m_f\bar\psi_f\psi_f$. It is understood that the vacuum expectation value has been subtracted in the matrix elements. Since hadrons are bound states of quarks and gluons, it is interesting to ask if one can learn more detailed information about the mass structure of hadrons in terms of the quark and gluon degrees of freedom. The partonic decomposition of hadron masses, in particular, the proton mass, has attracted a lot of attention lately both among the theory and experimental communities. On the theory side, the original proposal in [11] was to work in the rest frame of the hadron and decompose, at the operator level, the time component of the energy momentum tensor T^{00}. This leads to the formula

$$M = M_q^{\rm kin} + M_g^{\rm kin} + M_m + M_a, \tag{3}$$

where $M_{q/g}^{\rm kin}$ represents the kinetic and potential energy of quarks and gluons, M_m is from the quark mass term, and M_a is the trace anomaly contribution. While the decomposition (3) is gauge invariant, the choice of the component T^{00} inevitably brings up the issue of frame dependence. See [12] for a recent attempt to improve on this point.

In this paper, we propose another decomposition which is manifestly frame independent. Instead of decomposing M, one can decompose $M^2 = P^2$. The trace anomaly in (2) consists of the quark and gluon parts

$$T^\alpha_\alpha = (T_q)^\alpha_\alpha + (T_g)^\alpha_\alpha, \tag{4}$$

where

$$T_q^{\alpha\beta} = i\bar\psi\gamma^{(\alpha}D^{\beta)}\psi, \quad T_g^{\alpha\beta} = -F^{\alpha\lambda}F^\beta_\lambda + \frac{\eta^{\alpha\beta}}{4}F^2. \tag{5}$$

(The brackets denote symmetrization in indices.) We can thus write

$$M^2 = M_q^2 + M_g^2, \qquad M_{q,g}^2 = \frac{1}{2}\langle P|(T^R_{q,g})^\alpha_\alpha|P\rangle. \tag{6}$$

This decomposition makes sense as long as the operators $(T^R_{q,g})^\alpha_\alpha$ are carefully defined. They have to be regularized and renormalized in a certain regularization scheme, which means that the decomposition (6) is scheme dependent. (The sub- and superscript R stands for "renormalized.") While scheme dependence is always an issue no matter how one decomposes [for example, it is also relevant to (3)], the renormalization of $(T^R_q)^\alpha_\alpha$ and $(T^R_g)^\alpha_\alpha$ separately has been investigated only recently in [7,8], and so far only in dimensional regularization (DR) with the modified minimal subtraction $\overline{\rm MS}$ scheme. Let us briefly recapitulate the main results of [7,8]. In DR, at the bare operator level, the anomaly entirely comes from the gluon part of the energy momentum tensor

$$\langle P|(T_q)^\alpha_\alpha|P\rangle = \langle P|m\bar\psi\psi|P\rangle, \tag{7}$$

$$\begin{aligned}\langle P|(T_g)^\alpha_\alpha|P\rangle &= \langle P|\left(m\gamma_m\bar\psi\psi + \frac{\beta}{2g}F^2\right)|P\rangle \\ &= (0.637\alpha_s + \cdots)\langle P|m\bar\psi\psi|P\rangle \\ &\quad + (-0.3583\alpha_s + \cdots)\langle P|F^2|P\rangle,\end{aligned} \tag{8}$$

where we explicitly show the numerical value of the first term in the perturbative expansion of $\beta(g)/2g$ and $\gamma_m(g)$ for $N_c = 3$ and $n_f = 3$. Under renormalization, the coefficients of this expansion are reshuffled. This has been worked out to two loops in [7] and then extended to three loops in [8]. Here we quote the result of [8] for $N_c = 3$, $n_f = 3$,

$$\begin{aligned}\langle P|(T_{qR})^\alpha_\alpha|P\rangle &= \mathcal{C}_{qm}\langle P|(m\bar\psi\psi)_R|P\rangle \\ &\quad + \mathcal{C}_{qF}\langle P|(F^2)_R|P\rangle + \mathcal{O}(\alpha_s^4), \\ \langle P|(T_{gR})^\alpha_\alpha|P\rangle &= \mathcal{C}_{gm}\langle P|(m\bar\psi\psi)_R|P\rangle \\ &\quad + \mathcal{C}_{gF}\langle P|(F^2)_R|P\rangle + \mathcal{O}(\alpha_s^4),\end{aligned} \tag{9}$$

where

$$\begin{aligned}\mathcal{C}_{qm} &= 1 + 0.14147\alpha_s - 0.00823\alpha_s^2 - 0.06435\alpha_s^3, \\ \mathcal{C}_{qF} &= 0.07958\alpha_s + 0.05887\alpha_s^2 + 0.02160\alpha_s^3, \\ \mathcal{C}_{gm} &= 0.49515\alpha_s + 0.77659\alpha_s^2 + 0.86549\alpha_s^3, \\ \mathcal{C}_{gF} &= -0.43768\alpha_s - 0.26151\alpha_s^2 - 0.18383\alpha_s^3.\end{aligned} \tag{10}$$

In this formula, both the operators and the running coupling α_s are defined at some (perturbative) scale μ. Note that $m\bar{\psi}\psi = (m\bar{\psi}\psi)_R$ in DR, and the renormalization of the operator F_R^2 in this scheme is well understood in the literature [13].

Once the nonperturbative matrix elements $\langle P|F_R^2|P\rangle$ and $\langle P|(m\bar{\psi}\psi)_R|P\rangle$ are determined by some means, Eq. (6) together with (9) achieves a manifestly frame-independent, gauge-invariant decomposition of M^2. In the next sections, we shall discuss methods to experimentally constrain these matrix elements. As a preliminary, here we show how the matrix element of F_R^2 is related to the nucleon's gravitational form factors

$$\langle P'|(T^R_{q,g})^{\alpha\beta}|P\rangle = \bar{u}(P')\left[A^R_{q,g}\gamma^{(\alpha}\bar{P}^{\beta)} + B^R_{q,g}\frac{\bar{P}^{(\alpha}i\sigma^{\beta)\lambda}\Delta_\lambda}{2M} + C^R_{q,g}\frac{\Delta^\alpha\Delta^\beta - g^{\alpha\beta}\Delta^2}{M} + \bar{C}^R_{q,g}M\eta^{\alpha\beta}\right]u(P), \tag{11}$$

where $\bar{P}^\mu \equiv \frac{P^\mu + P'^\mu}{2}$ and $\Delta \equiv P' - P$. $D_{q,g} = 4C_{q,g}$ is often called the D-term. All the form factors depend on Δ^2, as well as the renormalization scale μ. Taking the trace of (11), we find

$$\langle P'|(T^R_{q,g})^{\alpha}_{\alpha}|P\rangle = \bar{u}(P')\left[A^R_{q,g}M + \frac{B^R_{q,g}}{4M}\Delta^2 - 3C^R_{q,g}\frac{\Delta^2}{M} + 4\bar{C}^R_{q,g}M\right]u(P). \tag{12}$$

Eliminating $m\bar{\psi}\psi$ from (9) and using (12), one finds

$$\langle P'|F_R^2|P\rangle = \bar{u}(P')\left[(K_gA^R_g + K_qA^R_q)M + \frac{K_gB^R_g + K_qB^R_q}{4M}\Delta^2 - 3\frac{\Delta^2}{M}(K_gC^R_g + K_qC^R_q) + 4(K_g\bar{C}^R_g + K_q\bar{C}^R_q)M\right]u(P), \tag{13}$$

where

$$K_g = \frac{1}{\mathcal{C}_{gF} - \frac{\mathcal{C}_{gm}}{\mathcal{C}_{qm}}\mathcal{C}_{qF}}, \qquad K_q = -\frac{\mathcal{C}_{gm}}{\mathcal{C}_{qm}}K_g. \tag{14}$$

Equation (13) is a useful formula which relates the nonforward matrix element of the operator F_R^2 to the gravitational form factors. The latter (excepting $\bar{C}_{q,g}$) have been calculated in lattice QCD simulations.

We also comment on the parameter b introduced in [11]

$$b \equiv \frac{\langle P|m(1+\gamma_m)(\bar{\psi}\psi)_R|P\rangle}{2M^2}, \quad 1-b = \frac{\langle P|\frac{\beta}{2g}(F^2)_R|P\rangle}{2M^2}. \tag{15}$$

Physically, b is the fraction of M^2 which comes from the current quark masses, analogous to the pion-nucleon sigma term $\sigma \sim \langle P|m\bar{\psi}\psi|P\rangle$. It is scheme and scale dependent so that one should more properly write $b \to b^R(\mu)$, though we keep the notation b below for simplicity. Taking the forward limit of (13) and using $\bar{C}_q = -\bar{C}_g$, we find the relation between b and the $\bar{C}_{q,g}$ form factor at zero momentum transfer

$$1 - b = \frac{\beta(g)}{2g}[(A^R_g(0) + 4\bar{C}^R_g(0))(K_g - K_q) + K_q]. \tag{16}$$

A recent $n_f = 2+1$ lattice calculation at the physical pion mass has found $\frac{\langle P|m(\bar{\psi}\psi)_R|P\rangle}{2M^2} \approx 0.09$ [14]. Since γ_m is positive, b is larger than this. A simple estimate gives $b \sim 0.12$.

III. J/Ψ PRODUCTION NEAR THRESHOLD AT JLAB

In this section, we update our previous calculation [3] of threshold J/ψ production from holography. The reason is threefold. First, we use the precise relation (13) between the matrix elements of F^2 and the gravitational form factors. In [3], the bare relation (8) has been used. Second, a lattice QCD calculation of the C_g-form factor is now available [9]. Third, very recently the Glue-X Collaboration at Jefferson Lab has reported new experimental data on the J/ψ photoproduction cross section near threshold [6]. In [3], we have fitted our result to the 40-year-old experimental data from Cornell and SLAC [4,5]. The new JLab data seem to be appreciably different from the Cornell data very close to the threshold.

Let us quickly review the discussion of [3]. The process of interest is the exclusive production of J/ψ in $ep \to e'\gamma p \to e'p'J/\psi$ near threshold. The intermediate photon state is nearly on shell (photoproduction) with the threshold energy $E_\gamma \approx 8.2$ GeV in the proton rest frame. Since QCD factorization has not yet been established for this process, the previous works employed various nonperturbative approaches [2,3,15–17]. In [3], two of the present authors proposed a holographic approach in which the scattering between the photon and the proton is described by the graviton and dilaton exchanges in five-dimensional anti–de Sitter space AdS_5. The dilaton is dual to the operator F^2 in gauge theory, so the cross section depends on the nonforward matrix element

$$\langle P'|F^2|P\rangle, \tag{17}$$

whose forward limit $P' \to P$ is related to the trace anomaly. But this limit is kinematically forbidden, and one has to perform an extrapolation $t = \Delta^2 \to 0$. References [2,15] assumed vector dominance for J/ψ and related the non-forward matrix element $\langle\gamma(q)|\ldots|J/\psi(k)\rangle$ to a forward matrix element $\langle J/\psi(k)|\ldots|J/\psi(k)\rangle$. However, the validity of vector dominance is unclear for J/ψ [18]. Moreover, the momentum transfer near threshold is rather large: at the threshold, $|\Delta| \sim 1.5$ GeV, and this is comparable to the charm quark mass which is treated as heavy. Instead, we tend to agree with the observation in [16,17] that the dependence on $t = \Delta^2$ should be that of "two-gluon" form factors, although the authors of [16,17] did not articulate what exactly these form factors are. Reference [3] explicitly showed that these are nothing but the gravitational form factors (11) and used the bare relation between $\langle F^2\rangle$ and A_g, B_g, C_g, $\bar{C}_g$. Here we revise the calculation in [3] by using the renormalized formula (13). Admittedly, this choice (bare or renormalized) is somewhat arbitrary and cannot be unambiguously settled in the framework of [3] which does not rely on QCD factorization. Our choice is pragmatic and mostly driven by the necessity to match the lattice QCD results on form factors which are usually presented in the $\overline{\rm MS}$ scheme. We note, however, that the difference between (13) and the one used in [3] is numerically not significant.

The cross section is computed as follows [3]. The scattering amplitude for the reaction $\gamma(q)p(P) \to p(P')J/\psi(k)$ is given by

$$\langle P|\epsilon\cdot J|P'k\rangle = X\bar{u}(P')[\Pi^{\mu\nu}\Gamma_{\mu\nu} + Y\Pi^{\mu}_{\mu}\Gamma]u(P), \tag{18}$$

where

$$\Pi^{\mu\nu}(q,k) \equiv q^{(\mu}k^{\nu)}\epsilon\cdot\xi + \epsilon^{(\mu}\xi^{\nu)}q\cdot k - q^{(\mu}\xi^{\nu)}k\cdot\epsilon - k^{(\mu}\epsilon^{\nu)}q\cdot\xi. \tag{19}$$

$q^\mu(k^\mu)$ and $\epsilon^\mu(\xi^\mu)$ correspond to the momentum and polarization for $\gamma(J/\psi)$. The first term corresponds to the graviton exchange, and the second term is from the dilaton exchange. We shall use the value $Y = -11/80$ from the model used in [3]. Explicitly [cf. (13)],

$$\Gamma^{\mu\nu} = (A_g^R + B_g^R)\gamma^{(\mu}\bar{P}^{\nu)} - \frac{\bar{P}^\mu\bar{P}^\nu}{M}B_g^R + \frac{1}{3}\left(\frac{\Delta^\mu\Delta^\nu}{\Delta^2} - \eta^{\mu\nu}\right)\left(A_g^R M + \frac{\Delta^2}{4M}B_g^R\right), \tag{20}$$

$$\Gamma = \frac{1}{4}\left[(K_g A_g^R + K_q A_q^R)M + \frac{K_g B_g^R + K_q B_q^R}{4M}\Delta^2 - 3\frac{\Delta^2}{M}(K_g C_g^R + K_q C_q^R) + 4(K_g\bar{C}_g^R + K_q\bar{C}_q^R)M\right]. \tag{21}$$

The differential cross section is given by

$$\frac{d\sigma}{dt} = \frac{\alpha_{\rm EM}}{4(W^2-M^2)^2}\frac{1}{2}\sum_{\rm pol}\frac{1}{2}\sum_{\rm spin}|\langle P|\epsilon\cdot J|P'k\rangle|^2, \tag{22}$$

where $W^2 = (P+q)^2$ and $\alpha_{\rm EM} = e^2/(4\pi)$. Equation (22) is proportional to an overall coefficient X^2 which is the only fitting parameter in our model.

We thus use the formula (13) with the following recent lattice QCD results for $A_g^R(t,\mu)$ and $C_g^R(t,\mu)$ with $n_f = 2+1$ at $\mu = 2$ GeV [9,19]

$$A_g^R(t,\mu) = \frac{0.58}{(1-t/m_A^2)^2}, \qquad C_g^R(t,\mu) = -\frac{7.2}{4(1-t/m_C^2)^3}, \tag{23}$$

with $m_A = 1.13$ GeV and $m_C = 0.76$ GeV.[1] As in [3], we set B_g to be zero because this form factor is known to be very small numerically. As for $\bar{C}_g^R$, we use the formula (16) and present the cross section as a function of the unknown parameter b defined in (15). The value of the running coupling is

$$\alpha_s(\mu = 2\ {\rm GeV}) = 0.30187, \tag{24}$$

evaluated in the same scheme as in [8].

In Fig. 1, we compare our result with the latest experimental data from the GlueX Collaboration [6]. The left panel is the energy dependence of the total cross section $\sigma_{\rm tot}$ where old experimental data points from Cornell [4] are also included. The right panel is the differential cross section $d\sigma/dt$ averaged over a narrow energy interval $10 < E_\gamma < 11.8$ GeV. The overall normalization is determined from the fit to $\sigma_{\rm tot}$, and the same normalization is used in $d\sigma/dt$. In [3], it was not possible to fit the Cornell data, so the authors tried to fit the SLAC data which are slightly at higher energies (i.e., further away from the threshold). However, the region of applicability of the formalism in [3] is really limited to low energies where the scattering amplitude is dominantly real. It is thus gratifying to see that we can now give a reasonable description of the new JLab data. As for $d\sigma/dt$, at $E_\gamma = 10.3$ GeV our model lies within the experimental error bars for both $b = 0$ and $b = 1$. However, the difference between $b = 0$ and $b = 1$ can be merely distinguished only when $-\delta t \approx 0$. When $E_\gamma > 10.6$ GeV, our result overshoots the measured cross section. In order to reach a better agreement (or disagreement) between our theoretical result and the experimental observation, it will be helpful to reduce the interval of

[1]Reference [9] also fitted the same lattice data in the dipole form $C_g^R(t,\mu) = -\frac{10}{4(1-t/m_C)^2}$ with $m_C = 0.48$ GeV. The two choices lead to very similar results. We note that several arguments suggest that the tripole form (23) is preferred [3,20,21].

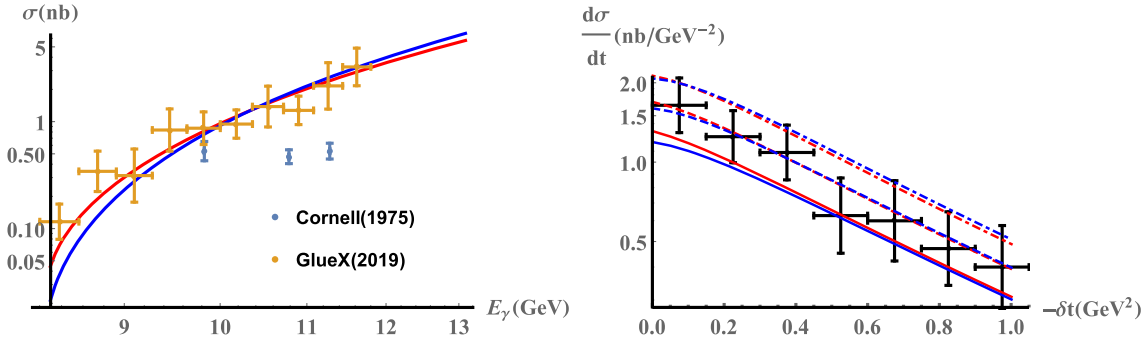

FIG. 1. (Left) Fits of the GlueX data [6] for the total cross section. The red curve corresponds to $b = 0$ and the blue curve corresponds to $b = 1$. (Right) Comparisons between the GlueX data [6] and our model for differential cross sections, where $\delta t = t - t_{\min}$. Color assignments are the same as the left panel, while the solid, dashed, and dot-dashed curves correspond to $E_\gamma = 10$, 10.3, and 10.6 GeV, respectively. The experimental data are taken for $10 < E_\gamma < 11.8$ GeV.

photon energy (say, $10 < E_\gamma < 10.6$ GeV). More importantly, as already noted in [3], it is highly desirable to go to even lower energies towards the threshold $E_\gamma = 8.2$ GeV, because then the difference between the red and blue curves becomes more pronounced.

From the fitting of the total cross section shown in the left panel, one also finds that the χ^2 deviation monotonically decreases when b is reduced within the expected range $0 \le b \le 1$. Consequently, the maximal anomaly scenario $b = 0$ [see (15)] yields the best fit. As a matter of fact, if we allow for negative b values, although this is at odds with the known sign of the nucleon sigma term, even better fits can be obtained. In Fig. 2, we plot χ^2 as a function of b. There is a shallow minimum around $b \sim -1$ and our model is not quite discriminative in the region $b \lesssim 0$. What we can clearly see, however, is that χ^2 increases steeply towards $b \to 1$, so the region $b \sim \mathcal{O}(1)$ is disfavored. This suggests that the F^2 term in the trace anomaly dominates over the quark mass term.

Following (9) and (15), we obtain

$$\frac{M_g^2}{M^2} = \left(\frac{\mathcal{C}_{gm} b}{1+\gamma_m(g)} + \frac{2g\mathcal{C}_{gF}(1-b)}{\beta(g)}\right) = 0.19b + 1.23(1-b), \tag{25}$$

with the three-loop formulas for $\gamma_m(g)$ and $\beta(g)$. When $b \le 0.22$, one finds $(M_g^R)^2 \ge M^2$ and thus $(M_q^R)^2 \le 0$. Such a scenario may be foreseen in (9) given $\langle P|(F^2)_R|P\rangle < 0$. We thus find that, quite interestingly, the quark part of the trace contributes negatively to the nucleon mass (in the present regularization scheme). This further emphasizes the role of gluons as the origin of the nucleon mass.

IV. THRESHOLD J/ψ AND Υ PRODUCTION IN ULTRAPERIPHERAL COLLISIONS AT RHIC

In this section, we demonstrate that the threshold production of J/ψ and Υ can be studied also at RHIC. At first sight, this may seem downright impossible since the RHIC energy $\sqrt{s} = 200$ GeV is too large to probe any threshold effects. Moreover, RHIC is a collider of protons and heavy nuclei, so superficially it has nothing to do with the physics of photoproduction.

However, it is well known that a heavy nucleus behaves as an abundant source of nearly on-shell photons, called Weizsäcker-Williams photons, in ultraperipheral collisions. A UPC is an event in which the impact parameter between the proton and the nucleus is so large that they can interact only via photons emitted from the nucleus. This process can therefore mimic the photoproduction limit of ep scattering. While the UPC event selection is not as clean as in the case of deep inelastic scattering photoproduction, the cross section is enhanced by Z^2, the atomic number squared of the nucleus which can be quite large $> \mathcal{O}(10^3)$. Moreover, at RHIC one can study the threshold production of Υ (the bound state of $b\bar{b}$) which cannot be done at JLab because the JLab energy (12 GeV in the proton rest frame) is below the Υ production threshold.

In UPCs, the cross section $pA \to p'A'J/\psi(k)$ or $pA \to p'A'\Upsilon(k)$ is related to the $p\gamma$ cross section through the standard formula

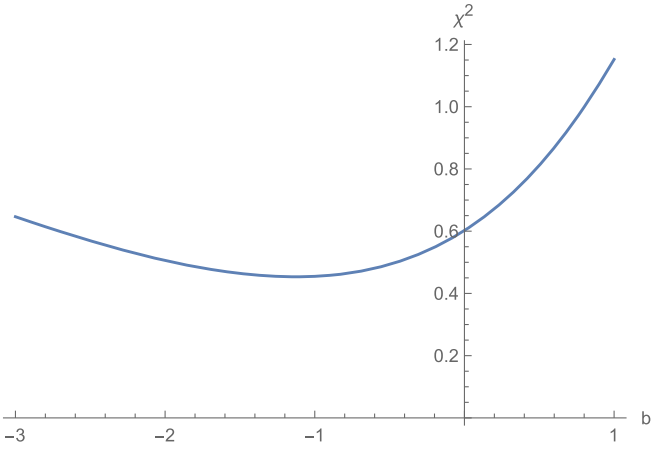

FIG. 2. χ^2 as a function of the parameter b.

$$\sigma^{pA} = \int d\omega \frac{dN}{d\omega}\sigma^{\gamma p}$$
$$= \int \frac{d^3k}{2E_k(2\pi)^3}\frac{d^3P'}{2E_{P'}(2\pi)^3}\frac{dN}{d\omega}\frac{e^2}{4MK}$$
$$\times (2\pi)^4\delta^{(3)}(\vec{P}+\vec{q}-\vec{P}'-\vec{k})|\langle P|\epsilon\cdot J|P'k\rangle|^2, \quad (26)$$

where $\omega = E_{P'} + E_k - E_P$ is the photon energy and

$$\frac{dN}{d\omega} = \frac{2Z^2\alpha_{em}}{\pi\omega}\left[\zeta K_0(\zeta)K_1(\zeta) - \frac{\zeta^2}{2}(K_1^2(\zeta) - K_0^2(\zeta)\right], \quad (27)$$

is the photon flux. We defined $\zeta = \omega\frac{R_p+R_A}{\gamma}$ and $K = \frac{W^2-M^2}{2M}$, with $W^2 = (P+q)^2$ being the $p\gamma$ center of mass energy. $R_{p/A}$ denotes the radius of the proton and nucleus. We consider pAu collisions at RHIC at $\sqrt{s_{NN}} =$ 200 GeV and work in the pp center-of-mass frame so that $Z = 79$, $\gamma = \sqrt{s_{NN}}/2M \approx 100$, $R_p \approx 1$ fm, and $R_A \approx 8$ fm. In this frame, $P^\mu = (E_P, 0, 0, P)$ $(E_P = \frac{\sqrt{s_{NN}}}{2})$ and $q^\mu = (\omega, 0, 0, -\omega)$.

The typical value of ω (from $\zeta \sim 1$) is $\omega \sim 2$ GeV which gives $W = \sqrt{(P+q)^2} \sim 28$ GeV. This is well above the Upsilon production threshold $W \sim 10$ GeV. Due to the asymmetry between the photon and proton energies, the produced quarkonium (Υ or J/ψ) with mass M_Q is typically found in the very forward region of the incident proton. Most of them are produced far away from the threshold. We need to identify the region of phase space corresponding to threshold production and zoom in on that region.

Integrating over $\vec{P}'$ in (26), we get

$$\sigma^{pA} = \frac{e^2}{64\pi^2 M}\int \frac{d^3k}{E_k}\frac{dN}{d\omega}\frac{1}{E_{P'}K}|\langle P|\epsilon\cdot J|P'k\rangle|^2, \quad (28)$$

where $E_{P'} = \sqrt{M^2+\vec{k}^2}$. In terms of the rapidity $y = \frac{1}{2}\ln\frac{E_k+k^3}{E_k-k^3}$ of the quarkonium, we have $d^3k/E_k = dyd^2k_\perp$ so that

$$\frac{d\sigma^{pA}}{dyd^2k_\perp} = \frac{e^2}{64\pi^2 M}\frac{dN}{d\omega}\frac{1}{E_{P'}K}|\langle P|\epsilon\cdot J|P'k\rangle|^2, \quad (29)$$

or after averaging over the azimuthal angle,

$$\frac{d\sigma^{pA}}{dydk_\perp^2} = \frac{\pi e^2}{64\pi^2 M}\frac{dN}{d\omega}\frac{1}{E_{P'}K}|\langle P|\epsilon\cdot J|P'k\rangle|^2. \quad (30)$$

In this formula,

$$E_{P'} = \sqrt{M^2 + k_\perp^2 + (P-\omega-M_Q^\perp\sinh y)^2},$$
$$\omega = \sqrt{M^2 + k_\perp^2 + (P-\omega-M_Q^\perp\sinh y)^2}$$
$$+ M_Q^\perp\cosh y - E_P, \quad (31)$$

where $M_Q^\perp = \sqrt{k_\perp^2 + M_Q^2}$. The second equation can be solved for ω and the result is

$$\omega = \frac{2M_Q^\perp(E_P\cosh y - P\sinh y) - M_Q^2}{2(E_p + P - M_Q^\perp e^y)}. \quad (32)$$

The threshold condition is

$$W^2 = M^2 + 2\omega(E_p+P) > (M+M_Q)^2$$
$$\to \omega > \frac{M_Q(2M+M_Q)}{2(E_P+P)} \approx \begin{cases} 0.27\ \text{GeV} & (\Upsilon) \\ 0.039\ \text{GeV} & (J/\psi) \end{cases}. \quad (33)$$

Therefore, the physical region for the kinematical variables $(y, k_\perp^2)$ is

$$\frac{2M_Q^\perp(E_P\cosh y - P\sinh y) - M_Q^2}{2(E_p + P - M_Q^\perp e^y)} - \frac{M_Q(2M+M_Q)}{2(E_P+P)} > 0. \quad (34)$$

In the left panel of Fig. 3, we plot the left-hand side of (34) for J/ψ, $M_Q = M_\psi = 3.10$ with $M = 0.94$, $E_P = 100$, $P = \sqrt{E_P^2 - M^2}$ (all in units of GeV). The threshold region is the lower-right corner around $y \lesssim 4$. The right panel is for Υ, $M_Q = M_\Upsilon = 9.46$.

In Fig. 4, left panel, we show the results of J/ψ production at $y = 3.8$. We use the same normalization factor as was used to fit the GlueX data with $b = 0$ in the previous section. We immediately notice that the magnitude of the cross section is quite large, thanks to the enhancement factor $Z^2 = 6241$. The difference between $b = 1$ and $b = 0$ becomes quite significant as $k_\perp \to 0$. In the right panel, we plot the ratio $d\sigma_{\text{pAR}} \equiv \left(\frac{d\hat{\sigma}_{pA}}{dydk_\perp^2}\right)_{b=0} / \left(\frac{d\hat{\sigma}_{pA}}{dydk_\perp^2}\right)_{b=1}$ at $k_\perp = 0.5$ GeV as a function of the rapidity y. This plot clearly shows that it is best to focus on the region $y \lesssim 4$.

In the case of Υ, we do not know the normalization factor, as X in (18) can depend on the quark mass.[2] Therefore, we plot the normalized differential cross sections $\hat{\sigma}_{\text{pA}} \equiv \sigma_{\text{pA}}/(\alpha_{\text{EM}}X^2)$ on the left panel of Fig. 5. In addition, on the right panel, we plot the ratio of $(d\hat{\sigma}_{pA})/(dydk_\perp^2)$ with $b = 0$ to with $b = 1$ at fixed $k_\perp$.

[2]If one assumes that the cross section scales as $\sigma \sim 1/m_q^2$, one has $\sigma_\Upsilon \sim 0.1\sigma_\psi$, which is not a strong suppression in view of the large Z^2 factor.

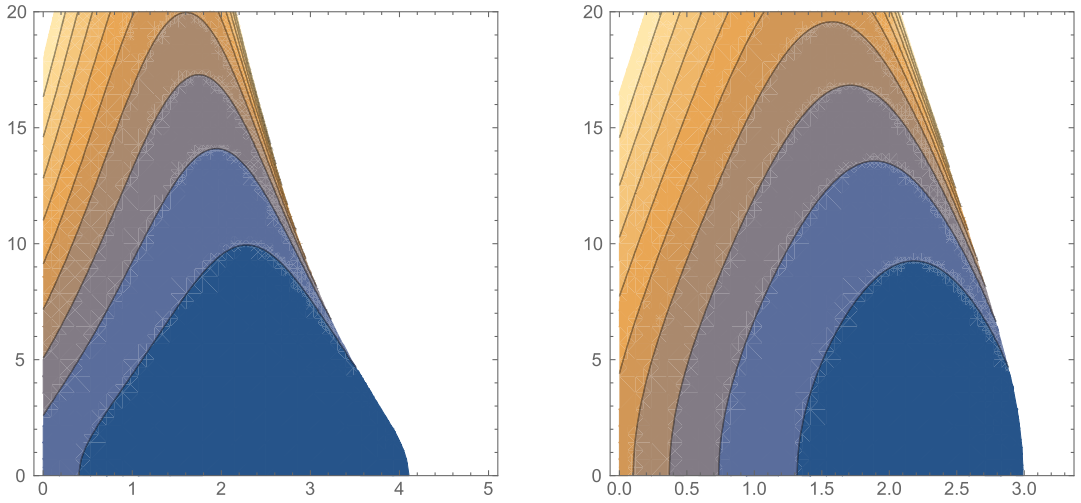

FIG. 3. Kinematically allowed region of J/ψ (left) and Υ (right). The horizontal axis is y and the vertical axis is $k_\perp$. The threshold region is in the lower-right corner.

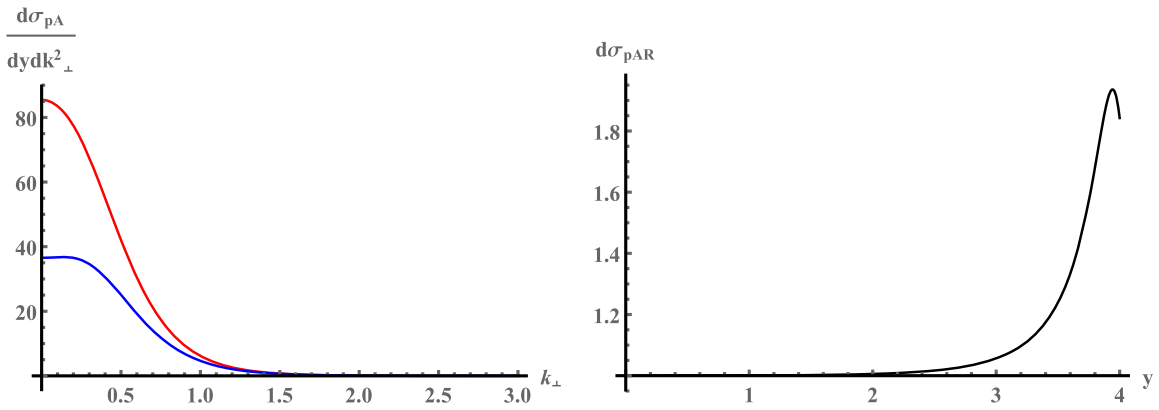

FIG. 4. (Left) The differential cross sections (nb GeV^{-2}) for J/ψ production in UPC at $y = 3.8$ with varying $k_\perp$ (GeV), where red and blue curves correspond to $b = 0$ and $b = 1$. (Right) The ratio of $d\sigma_{\mathrm{pAR}} \equiv (\frac{d\hat{\sigma}_{pA}}{dydk_\perp^2})_{b=0}/(\frac{d\hat{\sigma}_{pA}}{dydk_\perp^2})_{b=1}$ for J/ψ at $k_\perp = 0.5$ GeV.

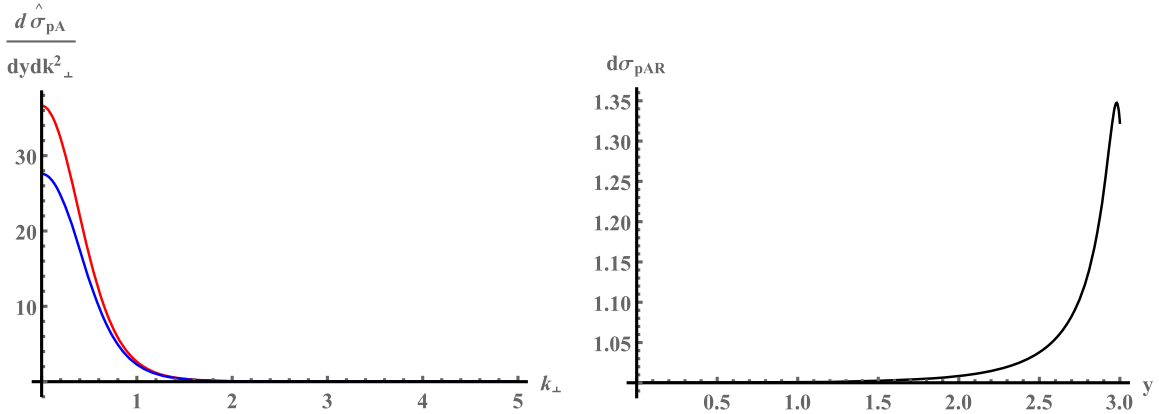

FIG. 5. (Left) The normalized differential cross sections for Υ production in UPC at $y = 2.9$ with varying $k_\perp$ (GeV), where red and blue curves correspond to $b = 0$ and $b = 1$. (Right) The ratio of $d\hat{\sigma}_{\mathrm{pAR}} \equiv (\frac{d\hat{\sigma}_{pA}}{dydk_\perp^2})_{b=0}/(\frac{d\hat{\sigma}_{pA}}{dydk_\perp^2})_{b=1}$ at $k_\perp = 0.5$ GeV.

It is found that the near threshold cross section is enhanced with the maximal anomaly at small $k_\perp$ and large rapidity. Qualitatively, the J/ψ production in UPC shares the similar properties as the case for Υ.

We finally note that with the STAR forward upgrade [10], which covers the pseudorapidity region $2.5 < \eta < 4$, the above measurement is feasible. Near the threshold, the produced quarkonium typically has high longitudinal momentum $k^3 \sim \mathcal{O}(E_p)$. It can be measured through its decay into a (massless) lepton pair. For a quarkonium with $k_\perp = 0$ and $k^3 = K$, the produced leptons have momentum $|k_\perp| = M_Q/2$ and $k^3 = K/2$ so that their pseudorapidity η is equal to the rapidity y of the parent quarkonium. Fortunately, the relevant values $y \lesssim 2.9$ and $y \lesssim 4$ for Υ and J/ψ, respectively, turn out to be perfectly within the coverage of the new detectors.

V. CONCLUSIONS

In this paper, we first updated our previous fit of the J/ψ photoproduction cross section in [3] in light of the new data from the GlueX Collaboration [6]. The quality of the fit has improved significantly, and we can now see a hint that the parameter b in (15) is small. This suggests that the gluon condensate $\sim\langle P|F^2|P\rangle$ dominates over the quark condensate $\langle P|m\bar{\psi}\psi|P\rangle$ in the QCD trace anomaly. In the alternative decomposition (6), it means that the quark part of the trace contributes negatively to the nucleon mass. This observation emphasizes more the role of gluons as the origin of the nucleon mass. On the other hand, our model is not discriminative enough to determine the value of b, and actually, negative values of b are allowed. To fix this problem, it would be very interesting to explore different holographic models from the one considered in [3].

We then demonstrated that the threshold production can be also studied in UPCs at RHIC in future. In addition to being complementary to the JLab measurements, a big advantage of RHIC is that one can study the threshold Υ production. The challenge is that one has to measure the quarkonia at very forward rapidities. However, this seems to be doable after the completion of planned forward upgrade of the STAR detectors.

Finally, it is worthwhile to comment that, although our main target in this paper has been the $\bar{C}_g$ form factor, the near threshold cross section is very sensitive to the gluon D-term

$$D_g^R(t,\mu) = 4C_g^R(t,\mu), \tag{35}$$

which has attracted considerable interest recently [22,23] in connection to the "pressure" or "radial force" inside the nucleon. This is because of the explicit prefactor Δ^2 in (13), and Δ is large near threshold. For the present purpose, the gluon D-term is an obstruction to precisely extract the $\bar{C}_g$ contribution. But turning the logic around, it may be possible to use the present processes to constrain the D-term which is poorly known experimentally. We leave this to future works.

ACKNOWLEDGMENTS

We thank Lubomir Pentchev, Mark Strikman, and Kazuhiro Tanaka for discussion and correspondence. This work is supported by the U.S. Department of Energy, Office of Science, Office of Nuclear Physics under Award No. DE-SC0012704. It is also supported by the LDRD program of Brookhaven National Laboratory. The work of D. Y. is partially supported by Keio Institute of Pure and Applied Sciences (KiPAS) project in Keio University and Yukawa International Program for Quark-hadron Sciences (YIPQS).

[1] S. Joosten and Z. E. Meziani, Proc. Sci. QCDEV2017 (**2018**) 017.
[2] D. Kharzeev, H. Satz, A. Syamtomov, and G. Zinovjev, Eur. Phys. J. C **9**, 459 (1999).
[3] Y. Hatta and D. L. Yang, Phys. Rev. D **98**, 074003 (2018).
[4] B. Gittelman, K. M. Hanson, D. Larson, E. Loh, A. Silverman, and G. Theodosiou, Phys. Rev. Lett. **35**, 1616 (1975).
[5] U. Camerini, J. G. Learned, R. Prepost, C. M. Spencer, D. E. Wiser, W. W. Ash, R. L. Anderson, D. M. Ritson, D. J. Sherden, and C. K. Sinclair, Phys. Rev. Lett. **35**, 483 (1975).
[6] A. Ali *et al.* (GlueX Collaboration), arXiv:1905.10811.
[7] Y. Hatta, A. Rajan, and K. Tanaka, J. High Energy Phys. 12 (2018) 008.
[8] K. Tanaka, J. High Energy Phys. 01 (2019) 120.
[9] P. E. Shanahan and W. Detmold, Phys. Rev. D **99**, 014511 (2019).
[10] STAR Collaboration, STAR Note 648, https://drupal.star.bnl.gov/STAR/starnotes/public/sn0648; Q. Yang (STAR Collaboration), Nucl. Phys. **A982**, 951 (2019).
[11] X. D. Ji, Phys. Rev. Lett. **74**, 1071 (1995).
[12] C. Lorcé, Eur. Phys. J. C **78**, 120 (2018).
[13] R. Tarrach, Nucl. Phys. **B196**, 45 (1982).
[14] Y. B. Yang, J. Liang, Y. J. Bi, Y. Chen, T. Draper, K. F. Liu, and Z. Liu, Phys. Rev. Lett. **121**, 212001 (2018).
[15] O. Gryniuk and M. Vanderhaeghen, Phys. Rev. D **94**, 074001 (2016).
[16] S. J. Brodsky, E. Chudakov, P. Hoyer, and J. M. Laget, Phys. Lett. B **498**, 23 (2001).

[17] L. Frankfurt and M. Strikman, Phys. Rev. D **66**, 031502 (2002).
[18] L. L. Frankfurt and M. I. Strikman, Nucl. Phys. **B250**, 143 (1985).
[19] P. E. Shanahan and W. Detmold, Phys. Rev. Lett. **122**, 072003 (2019).
[20] K. Tanaka, Phys. Rev. D **98**, 034009 (2018).
[21] C. Lorc, H. Moutarde, and A. P. Trawiski, Eur. Phys. J. C **79**, 89 (2019).
[22] V. D. Burkert, L. Elouadrhiri, and F. X. Girod, Nature (London) **557**, 396 (2018).
[23] M. V. Polyakov and P. Schweitzer, Int. J. Mod. Phys. A **33**, 1830025 (2018).